Title

19 F-Tagged metal binding pharmacophores for NMR screening of metalloenzymes

Journal

Chemical Communications, 57(40)

ISSN

1359-7345

Authors

Prosser, Kathleen E
Kohlbrand, Alysia J
Seo, Hyeonglim
et al.

Publication Date

2021-05-18

DOI

10.1039/d1cc01231b

Peer reviewed

HHS Public Access

Author manuscript

Chem Commun (Camb). Author manuscript; available in PMC 2022 May 18.

Published in final edited form as:

Chem Commun (Camb). 2021 May 18; 57(40): 4934–4937. doi:10.1039/d1cc01231b.

^{19}F-Tagged metal binding pharmacophores for NMR screening of metalloenzymes

Kathleen E. Prosser, **Alysia J. Kolhbrand**, **Hyeonglim Seo**, **Mark Kalaj**, **Seth M. Cohen***

Department of Chemistry and Biochemistry, University of California, San Diego, 9500 Gilman Drive, La Jolla, CA 92093

Abstract

This study demonstrates the screening of a collection of twelve ^{19}F-tagged metal-binding pharmacophores (MBPs) against the Zn(II)-dependent metalloenzyme human carbonic anhydrase II (hCAII) by ^{19}F NMR. The isomorphous replacement of Zn(II) by Co(II) in hCAII produces enhanced sensitivity and reveals the potential of ^{19}F NMR-based techniques for metalloenzyme ligand discovery.

Developing rapid and selective screening methods for bioactive small molecules continues to be an active area of investigation to identify pharmaceutical agents that act on established and emerging targets. An important target class is metalloproteins, wherein a metal ion, or ions, within a protein serves either structural or catalytic roles.[1–3] This work explores the use of ^{19}F NMR for the identification of small molecules that can bind to the metal ion in a metalloenzyme, which would be useful for ligand discovery against clinically relevant targets.

There are a variety of techniques used for the discovery and optimization of new small molecule pharmaceuticals, including high-throughput screening (HTS) and fragment-based drug discovery (FBDD).[45] FBDD utilizes low molecular weight (MW) molecules (<300 kDa) for screening and through synthetic elaboration strategies ultimately produces potent and more complete lead compounds.[6–8] FBDD has been applied specifically in the context of targeting metalloenzymes.[9, 10] A fragment library comprised of different metal-binding pharmacophores (MBPs) has been utilized to identify novel leads for bacterial,[11] viral,[3] and human[12] metalloenzymes and these MBP leads have been used to develop potent, selective inhibitors against this target class.[10]

* scohen@ucsd.edu.

Conflicts of interest

S.M.C. is a cofounder of and has an equity interest in Cleave Therapeutics and Forge Therapeutics, companies that may potentially benefit from the research results. S.M.C. also serves on the Scientific Advisory Board for Forge Therapeutics. The terms of this arrangement have been reviewed and approved by U.C. San Diego in accordance with its conflict of interest policies.

Electronic Supplementary Information (ESI) available: The Supporting Information is available free of charge on the ACS Publications website, includes fragment characterization and experimental details for ^{19}F NMR studies and X-ray crystallography. CCDC 2036941-2036943 contain the supplementary crystallographic data for this paper. These data can be obtained free of charge via www.ccdc.cam.ac.uk/data_request/cif, or by emailing data_request@ccdc.cam.ac.uk, or by contacting The Cambridge Crystallographic Data Centre, 12 Union Road, Cambridge CB2 1EZ, UK; fax +44 1223 336033.

In FBDD, a broad range of screening methods have been employed[13] that include biochemical assays, surface plasmon resonance (SPR), differential scanning fluorimetry (DSF), and structural methods including ligand- and protein-observed NMR.[14, 15] Protein-observed NMR typically requires expensive isotopic enrichment, while ligand-observed experiments can be performed with native protein, but provides less information.[13, 14] Ligand-observed screening can utilize traditional ^{1}H NMR, but the prevalence and convenient spectroscopic signal of fluorine has prompted extensive application of ^{19}F NMR,[16–22] particularly for fragment libraries.[23] For example, Dalvit and others have used ^{19}F NMR methods in a number of studies, including with kinases, which use Mg(II) as a co-factor, but do not have well defined metal active sites.[24] The fragments used in these kinase inhibitor studies are not metal binding fragments.[25] Indeed, the majority of Dalvit's work are focused on the use of ^{19}F-labeled substrates, such as three fluorine atoms for biochemical screening (3-FABS, and related n-FABs methods).[26, 27] This method involves the labeling of enzyme substrates with trifluoromethyl groups, where different ^{19}F NMR chemical shift values are observed for the substrate and product, thereby using the ^{19}F-labeled substrates for NMR-based enzyme activity screening. Although an interesting and important body of work, these studies have not explored the use of fluorine-labeled metal binding fragments for identifying lead scaffolds for metalloenzyme inhibitors.[28]

Herein, a proof-of-principle study on the application of ^{19}F NMR-based screening for identifying metalloenzyme-targeting fragments is presented. This represents a novel exploration of an MBP library for ^{19}F NMR studies and a new application of these studies specifically to metalloenzyme active sites. The findings here significantly expand the screening capabilities for MBP libraries through the generation of a library with spectroscopic handles suitable for NMR analysis. The metalloenzyme human carbonic anhydrase II (hCAII) was chosen as a model system due to the well-established metal active site and arylsulfonamides known as a privileged ligand class.[29] Metalloenzymes also provide the unique opportunity to explore metal substitution to alternative metalloforms, herein utilizing a paramagnetic Co(II) reconstituted hCAII. It is important to note that all of the experiments presented here were carried out on a standard 500 MHz NMR instrument, and as such can be carried out in most facilities without the need for high-end or specialized instrumentation (typically these experiments are performed with 600-800 MHz instruments using cryoprobes).[23] Furthermore, the most straightforward, 1D ^{19}F experiments were utilized to evaluate fragment binding to hCAII to demonstrate that this screening approach is accessible without the need for advance training in NMR pulse sequences and methodologies. The validity of these widely accessible NMR methods[16] was verified by enzyme activity and thermal shift assays. There are a number of additional NMR experiments that could be employed, including t_1 relaxation[30] and saturation transfer techniques,[31] among others,[24] that could further enable validation of fragment-protein interactions. However, these are beyond the scope of the present study, which seeks to demonstrate a simple and widely accessible alternative for fragment screening against metalloenzyme targets.

To carry out these studies a collection of 12 fluorinated MBPs were assembled (Figure 1a). These compounds were selected to obtain a diverse set of MBPs with a relatively small number of fragments, limited to molecules with a single ^{19}F fluoro- or trifluomethyl- group.

While -CF_3 groups are preferred because of their increased NMR signal intensity, they have greater steric bulk and are in some instances more challenging to prepare than their -F counterparts. For these proof-of-principle studies both -CF_3 and -F groups were included to validate their respective uses in future experiments. Fluorine has a large chemical shift anisotropy and the ^{19}F resonances for the collected MBP fragments range from −59 ppm (**12**) to −123 ppm (**4**) in 50 mM HEPES buffer at pH 8 (Figure 1b, Table S1). MBPs include the privileged hCAII arylsulfonamide scaffold (**9**), and compounds with poorer binding to hCAII, such as picolinic acid (**4**). The fluorinated collection also includes MBPs that possess a range of potential donor atoms (N, O, S), denticities (mono-, bi-dentate), and bite angles (4-, 5-, 6-membered rings). The diversity in MBPs and motifs was designed to explore and validate the application of a ^{19}F-MBP library for targeted metalloenzyme FBDD campaigns, and much larger libraries of fluorinated MBPs could be obtained with a modest synthetic effort and even from commercial sources.

Compound **9** was first titrated with hCAII (Figure S1) to determine the appropriate equivalents of protein for screening experiments. Compound **9** was selected because it is the privileged sulfonamide scaffold known to have tight binding to hCAII.[32] Change in the full-width half maximum (FWHM) of a given resonance was used as a quantitative metric to evaluate fragment binding. The change in linewidth of the ^{19}F resonance of **9** established that 0.2 equivalents of hCAII caused an 8% increase in linewidth (Table S2). A FWHM change of only 5% was observed with the apo-protein, consistent with significantly reduced fragment binding (Table S2). This validates that the changes observed in compound **9** resonance can be attributed Zn(II)-active site interactions.[16]

When all twelve ^{19}F MBPs are incubated together, most are well resolved, though compounds **2** and **9** have some signal overlap (Figure 1b). When 0.2 equivalents of hCAII is introduced to the mixture, only two resonances, those at −62.5 (**2** & **9**) and −61.7 (**11**), have FWHM increases >10%, 15%, and 11%, respectively (Table S3). The signal overlap of compounds **2** and **9** can be easily resolved to identify the true hit molecule(s) by screening a smaller subset of six fragments. Compounds were separated based on their chemical shifts with **1**, **3**, **6**, **9**, **11**, and **12** placed in one sample with the remaining compounds in a second sample. In this experiment, the FWHM of **9** changed by 29%, **11** by 21%, and **2** by only 7%, confirming the identity of the hit compounds as **9** and **11** (Table S3, Figure 2). Compounds **9** and **11** both have functional groups found in reported hCAII inhibitors.[29] The identity of compounds **9** and **11** as hits was validated by a colorimetric activity-based enzyme assay, in which compounds **9** and **11** resulted in 95% and 47% activity inhibition at a fragment concentration of 100 μM (Figure 2). Importantly, when the inhibitory activities of the ^{19}F-tagged fragments are compared to the changes in FWHM of ^{19}F resonances caused by incubation with hCAII, a strong positive correlation was observed (Figure S10). An additional ^{19}F NMR experiment with bovine serum albumin (BSA), a protein with several non-specific hydrophobic binding pockets, results in nine out of the twelve compounds in Figure 1 producing changes in FWHM >10% (Figure S2). These experiments demonstrate the selectivity of the hCAII ^{19}F NMR screening; the platform correctly identifies two MBPs from a mixture of twelve compounds and is more selective for MBPs when compared to screening against a non-metalloprotein.

It is typical when screening by ^{19}F NMR to perform a competition experiment with a known inhibitor if one is available. Such assays validate that ^{19}F-tagged hit interacts with the desired binding site of the protein. Acetazolamide has a reported K_d of 20 nM for hCAII, providing a strong, unlabeled inhibitor for an ^{19}F NMR-based competition experiment.[32] Compound **9** (300 μM) was incubated with hCAII (100 μM) to produce a 16% increase in ^{19}F resonance FWHM. A titration with increasing equivalents of acetazolamide (0 – 300 μM) recovered the linewidth of **9** to only a 2% residual change by displacing the labeled fragment from the active site (Figures S4–5). This demonstrates that methods applied to traditional NMR screening can be utilized to validate active site binding by ^{19}F-tagged MBPs.

In prior FBDD campaigns with MBPs, initial screening is utilized to identify if a given fragment inhibits a particular metalloenzyme of interest. Therefore, it would be beneficial to correlate the activity and binding of fluorinated and non-fluorinated MBPs. This issue may be uniquely problematic to MBPs because the significant electron withdrawing effects of fluorine may negatively impact the metal coordinating ability of the fragments. The suitability of the ^{19}F MBPs to act as surrogates for MBPs more broadly was confirmed by comparing inhibitory behavior of the fluorinated (**1-12**) and non-fluorinated molecules (**1a**-**4a** versus **7a**-**11a**, Figure S7). In these assays the fluorinated and non-fluorinated molecules produced similar inhibition of hCAII (Figure S8–9) with a strong positive correlation coefficient of 0.92. In addition, the coordination of compounds **4** and **4a,** and **9** and **9a** were compared using a well-established Tp^{Ph,Me}Zn(MBP) model complex (Tp^{Ph,Me} = hydrotris(5,3-methylphenylpyrazolyl)borate))).[33] The metal binding mode of the fluorinated and non-fluorinated MBPs are nearly identical upon comparing the bond lengths and angles as determined by X-ray crystallography (Figures S11–12, Tables S5–6). A small lengthening of the pyridine-Zn(II) bond is observed for compound **4** over **4a** as would be expected due to the direct ring substitution leading to the largest electron withdrawing effect. These results suggest that -CF_3 substituents may be more desirable for both the enhanced NMR signal intensity and reduced electronic effects, although they may have may result in undesirable steric effects[34] when compared to monofluorinated compounds.

A tool uniquely available to metalloproteins is the substitution of metal ions in the active site for those that can modulate activity, structure, and spectroscopic features. It is common to exchange spectroscopically silent Zn(II) for spectroscopically active Co(II). For the studies here, the introduction of a paramagnetic Co(II) ion to the enzyme active site introduces paramagnetic relaxation enhancement (PRE) to the observable effects on nearby ^{19}F nuclei. PRE depends significantly on proximity ($1/r^6$),[35] so any interactions with distant residues on the protein would not result in any additional line broadening effects compared to a diamagnetic sample. To validate the suitability of a paramagnetic metalloprotein for ^{19}F NMR screening, a Co(II)-hCAII sample with 90%-Co(II)/10%-Zn(II) in the active site (confirmed by ICP-MS) was titrated with against compound **9** (Figure S6). When compared to the Zn(II) sample, a 2-fold greater change in linewidth was observed for the Co(II) sample (Figure 3). Only 0.1 equivalents of Co(II)-hCAII was required to induce a 9% increase while at 0.2 equivalents of protein a 15% increase in FWHM was observed. A control experiment with $CoCl_2$ found that 0.2 equivalents of the paramagnetic ions in solution caused only a 6%

increase in linewidth, indicating that the presence of Co(II) alone cannot account for all the line broadening observed in the protein sample (Table S2). This experiment demonstrates that paramagnetic active sites can be used to validate binding to the metalloenzyme active site using ^{19}F-tagged MBPs, as no difference would have been observed between the paramagnetic and diamagnetic samples if the fragment was interacting with distant protein sites. These data also indicate that ^{19}F NMR-based screening of MBPs could be carried out with paramagnetic metalloenzymes, such as the Mn(II) containing endonuclease,[3] with lower protein concentrations than what is required of diamagnetic proteins due to the combined effects of protein binding and PRE.

Together, these experiments demonstrate the suitability of ^{19}F NMR for the screening and identification of MBPs for metalloenzyme inhibitor development. When ^{19}F-tagged MBPs are incubated with hCAII known inhibitor scaffolds were correctly identified by examining changes in resonance FWHM. The comparison of activity and thermal shift assays, as well as Zn(II) model complex structures, highlights that these fluorinated molecules serve as suitable analogues to their non-fluorinated counterpoints, allowing for the extrapolation of screening results to inhibitor development. The proof-of-concept collection of fragments presented here can readily be expanded to include different metal binding motifs suitable for a diverse collection of therapeutically relevant metalloproteins. Furthermore, we have highlighted the unique advantage of targeting metal active sites, principally the properties afforded by the generation of alternative protein metalloforms and use of conventional, readily available spectrometers and simple data collection and analysis methods.

Supplementary Material

Refer to Web version on PubMed Central for supplementary material.

Acknowledgements

This work was supported by the National Institutes of Health (R21 AI138934; R01 AI149444), a Natural Sciences and Engineering and Research Council of Canada Postdoctoral Fellowship (K.E.P.), a Department of Defense National Defense Science and Engineering Graduate Fellowship and Achievement Rewards for College Scientists Foundation fellowship (M.K.). We gratefully acknowledge support from the UCSD Department of Chemistry & Biochemistry crystallography facility, and Dr. Neal Arakawa of the UCSD ECAL Facility for collecting ICP-MS data.

Notes and references

1. Chen AY, Adamek RN, Dick BL, Credille CV, Morrison CN and Cohen SM, Chem. Rev, 2019, 119, 1323–1455. [PubMed: 30192523]
2. Méplan C, Richard M-J and Hainaut P, Oncogene, 2000, 19, 5227–5236. [PubMed: 11077439]
3. Credille CV, Chen Y and Cohen SM, J. Med. Chem, 2016, 59, 6444–6454. [PubMed: 27291165]
4. Macarron R, Banks MN, Bojanic D, Burns DJ, Cirovic DA, Garyantes T, Green DVS, Hertzberg RP, Janzen WP, Paslay JW, Schopfer U and Sittampalam GS, Nat. Rev. Drug Discovery, 2011, 10, 188–195. [PubMed: 21358738]
5. Lloyd MD, J. Med. Chem, 2020, DOI: 10.1021/acs.jmedchem.0c00523.
6. Murray CW and Rees DC, Nat. Chem, 2009, 1, 187–192. [PubMed: 21378847]
7. Morrison CN, Prosser KE, Stokes RW, Cordes A, Metzler-Nolte N and Cohen SM, Chemical Science, 2020, 11, 1216–1225.

8. Keserű GM, Erlanson DA, Ferenczy GG, Hann MM, Murray CW and Pickett SD, J. Med. Chem, 2016, 59, 8189–8206. [PubMed: 27124799]
9. Jacobsen JA, Fullagar JL, Miller MT and Cohen SM, J. Med. Chem, 2011, 54, 591–602. [PubMed: 21189019]
10. Cohen SM, Acc. Chem. Res, 2017, 50, 2007–2016. [PubMed: 28715203]
11. Chen AY, Thomas CA, Thomas PW, Yang K, Cheng Z, Fast W, Crowder MW and Cohen SM, ChemMedChem, 2020, 15, 1272–1282. [PubMed: 32315115]
12. Perez C, Barkley-Levenson AM, Dick BL, Glatt PF, Martinez Y, Siegel D, Momper JD, Palmer AA and Cohen SM, J. Med. Chem, 2019, 62, 1609–1625. [PubMed: 30628789]
13. Renaud J-P, Chung C.-w., Danielson UH, Egner U, Hennig M, Hubbard RE and Nar H, Nat. Rev. Drug Discovery, 2016, 15, 679–698. [PubMed: 27516170]
14. Hubbard RE and Murray JB, in Methods Enzymol., ed. Kuo LC, Academic Press, 2011, vol. 493, pp. 509–531.
15. Carr RAE, Congreve M, Murray CW and Rees DC, Drug Discovery Today, 2005, 10, 987–992. [PubMed: 16023057]
16. Tengel T, Fex T, Emtenäs H, Almqvist F, Sethson I and Kihlberg J, Org. Biomol. Chem, 2004, 2, 725–731. [PubMed: 14985813]
17. Dalvit C, Mongelli N, Papeo G, Giordano P, Veronesi M, Moskau D and Kümmerle R, J. Am. Chem. Soc, 2005, 127, 13380–13385. [PubMed: 16173772]
18. Vulpetti A and Dalvit C, ChemMedChem, 2013, 8, 2057–2069. [PubMed: 24127294]
19. Zimmermann K, Joss D, Müntener T, Nogueira ES, Schäfer M, Knörr L, Monnard FW and Häussinger D, Chem. Sci, 2019, 10, 5064–5072. [PubMed: 31183057]
20. Jordan JB, Poppe L, Xia X, Cheng AC, Sun Y, Michelsen K, Eastwood H, Schnier PD, Nixey T and Zhong W, J. Med. Chem, 2012, 55, 678–687. [PubMed: 22165820]
21. Cobb SL and Murphy CD, J. Fluorine Chem, 2009, 130, 132–143.
22. de Castro GV and Ciulli A, Chem. Commun, 2019, 55, 1482–1485.
23. Troelsen NS, Shanina E, Gonzalez-Romero D, Danková D, Jensen ISA, Śniady KJ, Nami F, Zhang H, Rademacher C, Cuenda A, Gotfredsen CH and Clausen MH, Angew. Chem., Int. Ed, 2020, 59, 2204–2210.
24. Dalvit C and Vulpetti A, J. Med. Chem, 2019, 62, 2218–2244. [PubMed: 30295487]
25. Nagatoishi S, Yamaguchi S, Katoh E, Kajita K, Yokotagawa T, Kanai S, Furuya T and Tsumoto K, Bioorg. Med. Chem, 2018, 26, 1929–1938. [PubMed: 29510947]
26. Dalvit C, Veronesi M and Vulpetti A, J. Biomol. NMR, 2020, 74, 613–631. [PubMed: 32347447]
27. Dalvit C, Ardini E, Fogliatto GP, Mongelli N and Veronesi M, Drug Discovery Today, 2004, 9, 595–602. [PubMed: 15239978]
28. Forino M, Johnson S, Wong TY, Rozanov DV, Savinov AY, Li W, Fattorusso R, Becattini B, Orry AJ, Jung D, Abagyan RA, Smith JW, Alibek K, Liddington RC, Strongin AY and Pellecchia M, Proc. Natl. Acad. Sci. USA, 2005, 102, 9499–9504. [PubMed: 15983377]
29. Martin DP, Hann ZS and Cohen SM, Inorg. Chem, 2013, 52, 12207–12215. [PubMed: 23706138]
30. Dalvit C and Piotto M, Magn. Reson. Chem, 2017, 55, 106–114. [PubMed: 27514284]
31. Mayer M and Meyer B, J. Am. Chem. Soc, 2001, 123, 6108–6117. [PubMed: 11414845]
32. Iyer R, Barrese AA, Parakh S, Parker CN and Tripp BC, J. Biomol. Screening, 2006, 11, 782–791.
33. Jacobsen FE, Lewis JA and Cohen SM, J. Am. Chem. Soc, 2006, 128, 3156–3157. [PubMed: 16522091]
34. Jagodzinska M, Huguenot F, Candiani G and Zanda M, ChemMedChem, 2009, 4, 49–51. [PubMed: 19065645]
35. Clore GM and Iwahara J, Chem. Rev, 2009, 109, 4108–4139. [PubMed: 19522502]

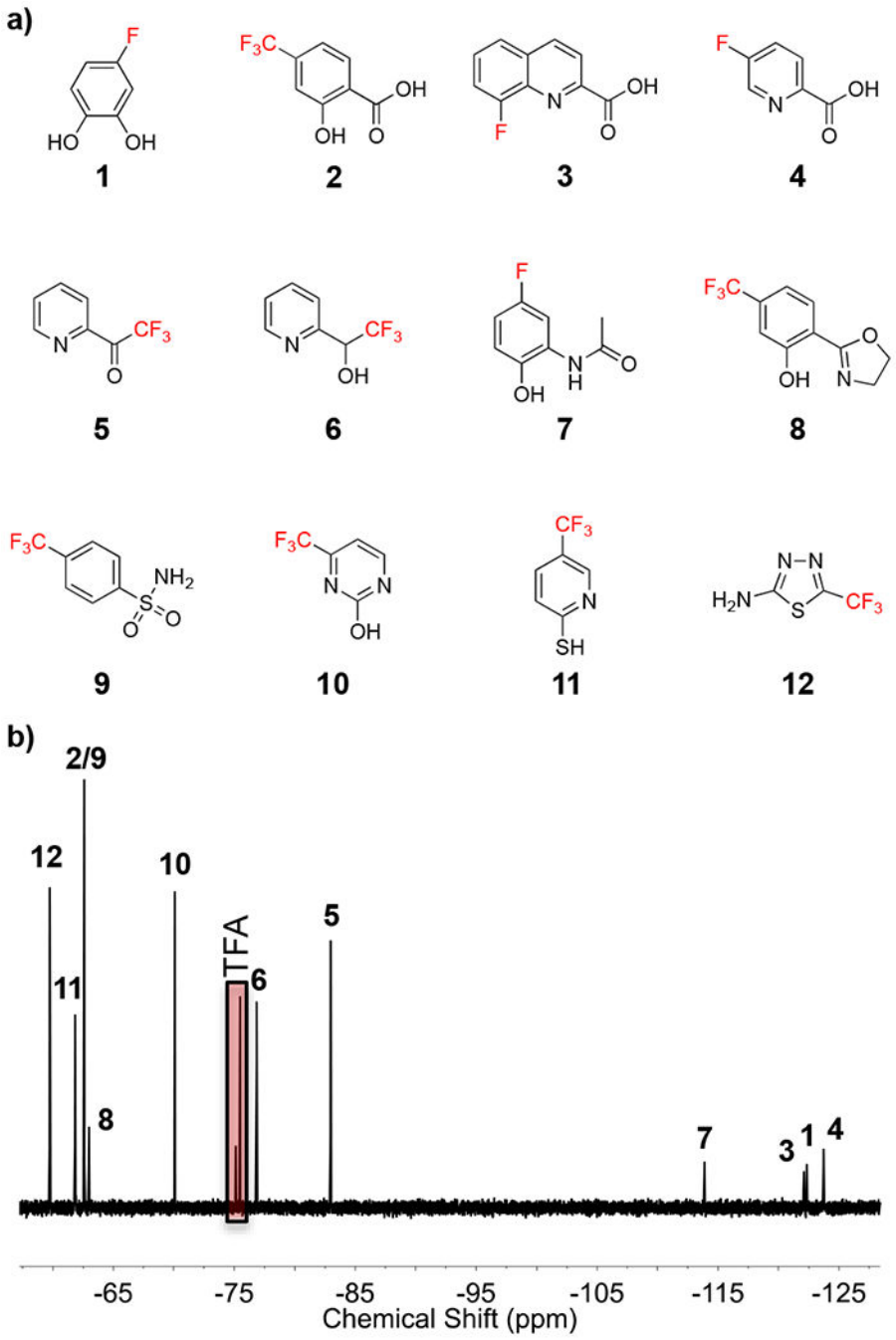

Figure 1.

a) The collection of fluorinated MBPs used to validate ^{19}F NMR screening in this study and b) the ^{19}F NMR spectrum of all 12 MBPs dissolved in 50 mM HEPES buffer pH 8.

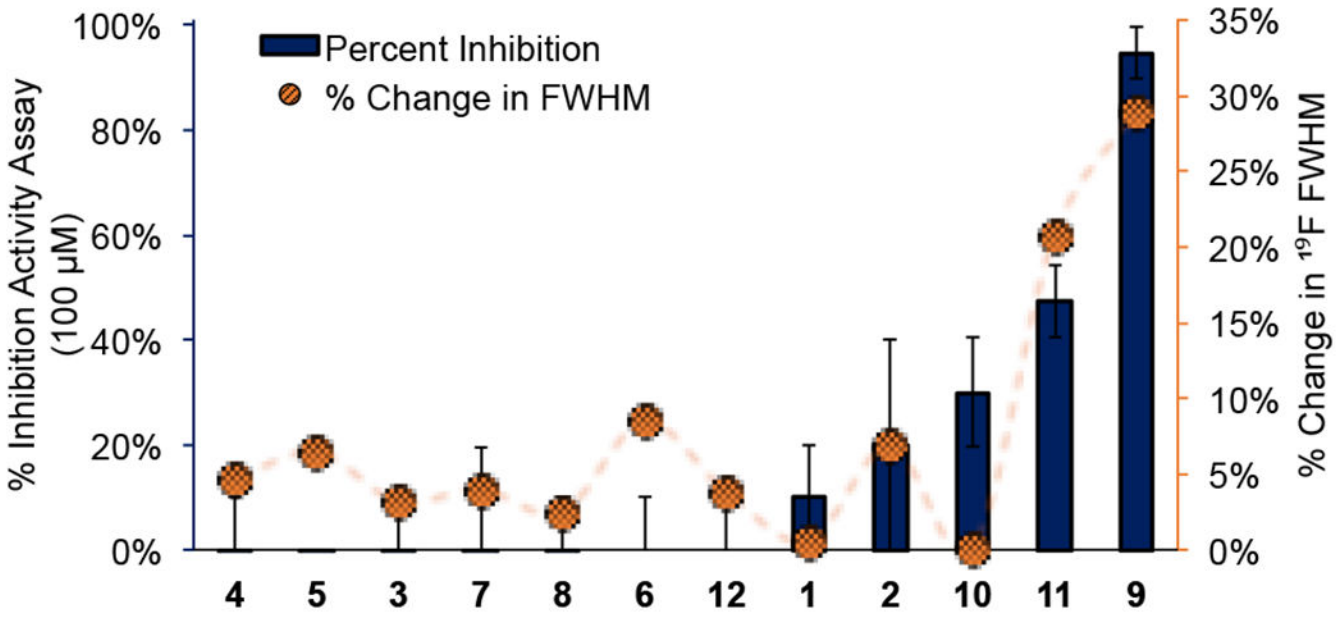

Figure 2.

The percent inhibition of hCAII by compounds **1**-**12** tested at 100 μM, and changes in ^{19}F NMR linewidth for the same compounds when incubated with hCAII.

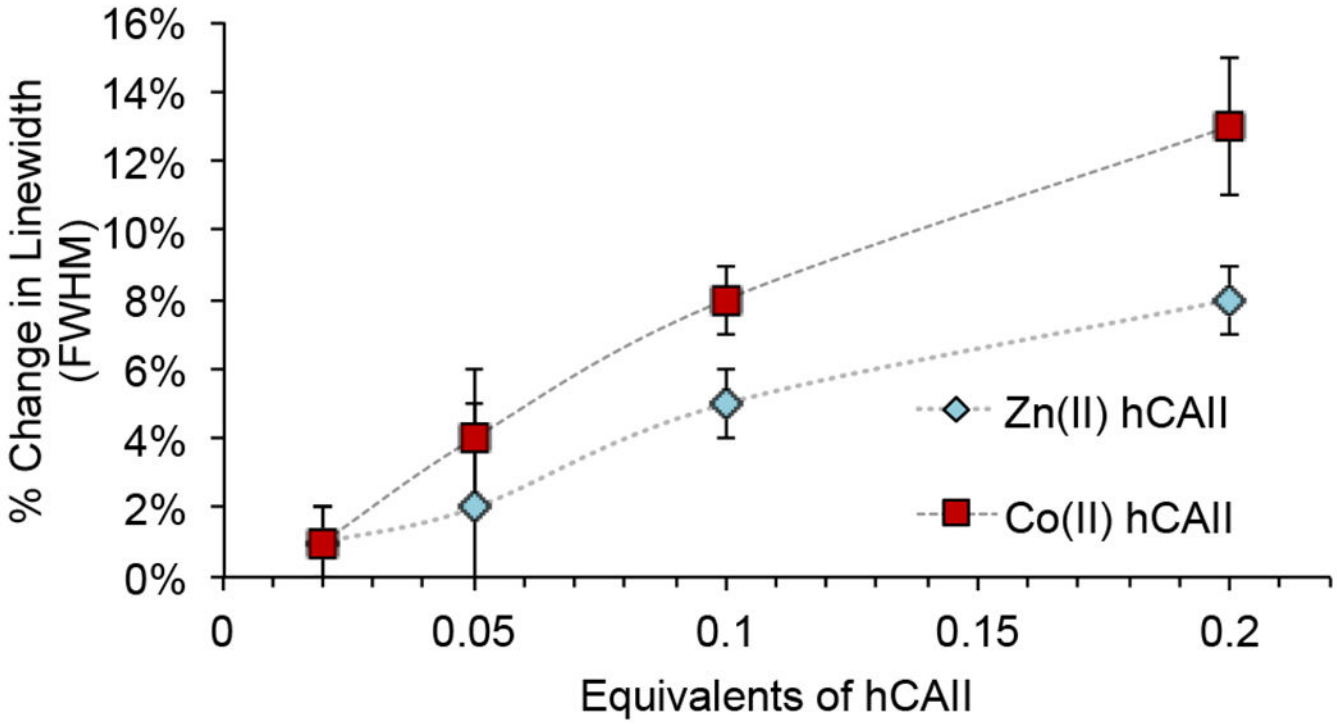

Figure 3.

The percent change in the FWHM of the ^{19}F NMR resonance of compound **9** when incubated with Zn(II)-hCAII is less than the change induced by the same equivalents the Co(II)-hCAII construct.